24-032

Enhancement of Ultrafine Phosphate Flotation Using Eriez' Cavtube Column Flotation Technology

Maoming Fan
Eriez Flotation, Erie, PA, USA

Rahul Singh
Eriez Flotation, Erie, PA, USA

Sunil Kumar
Industries Chimiques du Senegal (ICS), Dakar, Senegal

Erich Dohm
Eriez Flotation, Erie, PA, USA

ABSTRACT

The rapid increase of P_2O_5 use for food, biofuels, and $LiFePO_4$ batteries etc. accelerates the depletion rate of phosphate reserves. In the phosphate industry, a significant amount of ultrafine phosphate has been discarded as slime tailing due to processing difficulties. The major problems associated with ultrafine particle flotation are low probability of bubble-particle collision and adhesion, and high probability of unwanted gangue particles entrainment. This paper investigates the enhanced ultrafine phosphate particle flotation probability by Eriez' CavTube generated fine/ultrafine bubbles and the improved flotation selectivity by wash water etc. Ultrafine phosphates with various gangue minerals of quartz/muscovite, calcite/dolomite, and iron/silica were studied. Microscopic observations show that the entrained ultrafine gangue minerals can be minimized by using wash water in column flotation. A three-factor three-level central composite experimental design was conducted for ultrafine phosphate flotation. For comparison, both benchtop mechanical cell and laboratory column flotation tests were performed at their optimal respective flotation conditions. Using Eriez CavTube column flotation technology for Industries Chimiques du Senegal (ICS) ultrafine slime tailings, a concentrate grade of 36.0% P_2O_5, was achieved at 89.4% P_2O_5 recovery. Improved flotation performance was achieved using column flotation as compared to benchtop mechanical cell flotation. The benefits of Eriez' column flotation technology realized from this study include the high P_2O_5 grade and recovery.

INTRODUCTION

Phosphate is crucial for plants and animals, including humans. Isaac Asimov, an important science writer, defined phosphorus as "life's bottleneck." The rapid increase in P_2O_5 use is mainly caused by the growth in demand for food because, coupled with increased food crops for biofuels and the great demand for $LiFePO_4$ batteries, etc. In many phosphate mines, a significant amount of phosphate is routinely discarded as an ultrafine slime tailing stream due to technical and economic barriers using conventional flotation technology. Ultrafine particle flotation has been a long-standing problem, especially for non-sulfide ores flotation. The major issues associated with ultrafine particle flotation are the low probability of bubble-particle collision, the low probability of bubble-particle adhesion, and the high probability of unwanted gangue particles entrainment.

In the past twenty years, scholars have conducted extensive scientific work to improve fine/ultrafine particle flotation using fine and ultrafine bubbles generated by hydrodynamic cavitation [1–20]. Ultrafine bubbles can bridge hydrophobic particles to form aggregates [21–23] and increase the ultrafine particles flotation selectivity and flotation kinetics. Cavitation tube generated nanobubbles can not only promote the formation of flocs, but also increase the stability of flocs [24–28]. Improved flotation performance by cavitation tube generated fine bubbles has been verified in the flotation of various minerals such as quartz [29–33], sulfide [34–41], phosphate [42–46], coal

[8, 47–55], graphite [56–59], calcite [60], bitumen and oil [61–67], muscovite [68], kaolinite [69], wolframite [70], magnesite [71], PGM-bearing ore [72], niobium [73], serpentine [74], ions [75], wastewater treatment [76–85], fly ash [86], and spent batteries [87], etc. Extensive fundamental research has been done to improve the understanding of cavitation generated nanobubble/microbubble [4–8, 47, 88–108] on various applications.

Over 1,000 Eriez flotation columns with a variety of sparging technologies have been installed for floating quartz from iron ore, various kinds of sulfide minerals, gold, phosphate, coal, graphite, bauxite, calcite, bitumen, kaolinite, PGM-bearing ore, niobium, potash, and oil/water, etc. Typically, flotation columns produce higher grade and have lower operating costs than conventional mechanical cells.

Figure 1 shows Eriez' CavTube flotation column. Flotation column cells function as three phase settlers where particles move downwards in a hindered settling environment counter-current to a flux of rising air bubbles, which are generated by spargers located near the bottom of the cell. The sparger technology is an important design choice and allows the user to optimize the performance based on the feed characteristics, such as particle size distribution, liberation class and floatability, etc. Eriez can recommend and design the most appropriate equipment for the specific application.

The mechanism of particle/bubble collision in columns is different from intensive mixing devices such as mechanically agitated cells. Under the low intensity mixing caused only by a rising bubble field, particle drifting from the fluid streamlines is caused by gravity and inertial forces and by interception. A column can support a deep froth bed and may use wash water to maintain a downward flow of water (positive bias) evenly across the cross-section of the vessel. This eliminates the entrainment of hydrophilic particles in the float product when the vessel is used for solid/solid separation. This property, along with the absence of bypass of feed material to the float product from turbulence, means that column cells are normally superior to impeller type machines for the selective separation of ultrafine/fine particles (high grade).

This paper investigates the effects of flotation column wash water rate, feed solids content, and feed particle size distribution on the product P_2O_5 grade and P_2O_5 recovery of an ultrafine phosphate flotation. A three-level three-factor central composite experimental design was employed for investigating these three parameters for improving ultrafine phosphate flotation selectivity. For comparison, both benchtop Denver cell and laboratory column flotation tests were performed at their respective optimal flotation conditions. Various kinds of phosphate ores with the gangue minerals composed of quartz/muscovite, calcite/dolomite, and iron/silica were studied using CavTube generated fine and ultrafine bubbles.

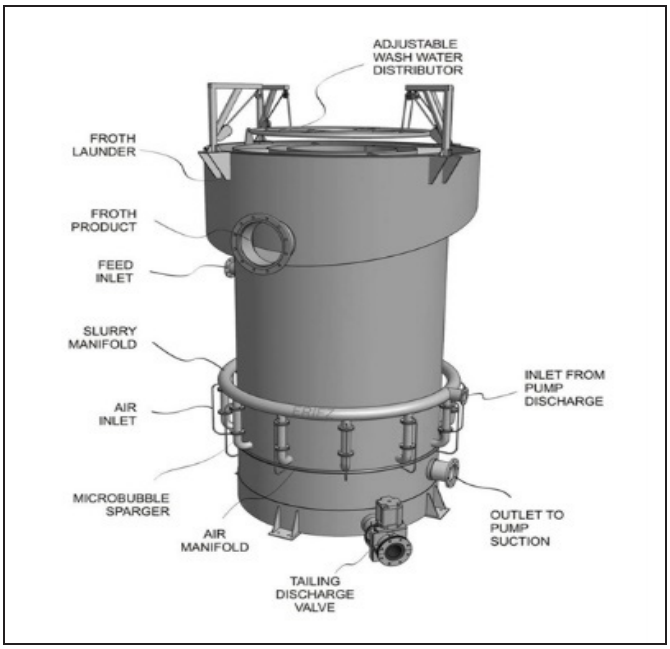

Figure 1. Illustration of Eriez CavTube flotation column

MATERIALS AND METHODS

Three(3) separate studies were carried out in this investigation, including microscopic observations of ultrafine phosphate slime flotation froth with and without wash water, the three-factor three-level experimental design, and the column vs. mechanical cell comparison flotation. A Celestron 44348 LCD digital microscope was used for microscopic observation study. A S3500 MicroTrac particle size analyzer using laser diffraction was employed to measure the feed particle size distribution.

Table 1 shows the three-factor three-level central composite experimental design conducted for ultrafine phosphate column flotation tests using the Design-Expert software acquired from Stat-Ease Inc., Minneapolis, MN. Three process parameters included froth wash water flow rate, feed slurry solids content, and feed particle size (P_{80}).

Each numeric factor shown in Table 1 and Table 2 varies over three levels: plus 1 and minus 1 (factorial points) and the center point. The levels of process variables were coded as "–1" "0" and "+1," respectively, where "–" represents the low level, "0" represents the middle level and "+" represents the high level of the factors. The specific levels of individual variables are indicated in Table 1. The details of designed experiments are shown in Table 2.

Table 1. Variables for three-factor three-level design

Levels		Factors and Values A Washwater (Liter/Minute)	B Feed P80 (Micron)	C Feed Solids (%)
Low	-1	0	20	10
Middle	0	400	38	17.5
High	1	800	53	25

A Denver, D12 laboratory flotation machine employed for benchtop flotation tests, while 3-inch (75 mm) diameter Eriez laboratory-scale flotation columns was used in batch-continuous operation to investigate the column flotation response. During benchtop flotation tests, the pH level was adjusted to approximately 9.5 using a 10% NaOH solution in rougher direct flotation conditioning. The feed was conditioned at 50–65% solids for 2 minutes with sodium silicate, 1 minute with starch, and finally 2 minutes with collector.

Figure 2 schematically shows the Eriez laboratory scale flotation column. Eriez laboratory columns utilize an Eriez CavTube sparging system, which consists of an in-line sparging device that works in conjunction with a recycle pump. The pump withdraws pulp from the base of the column and distributes it through the sparger. Air is added to the pulp prior to the sparger and then injected back into the column flotation cell. The high shear and cavitation induced into the liquid flow as it passes through the CavTube creates a fine bubble dispersion for particle collection and is especially effective for treatment of fine material. The column cell test assembly is fully automated. During completion of each test, the froth level was maintained through the use of a PID loop controller, in conjunction with a pressure transducer and an electronic peristaltic underflow pump. Manual air and wash water flow meters were also present for control of those operating parameters. A polyglycol frother was injected into the column cell through the use of a peristaltic chemical metering pump.

The column feed was prepared by transferring a weighed amount of solid material into a 20-gallon agitated feed slurry tank, followed by the addition of tap water to attain the desired percent solids and adjustment of pH level to approximately 9.5 using a 10% NaOH solution. The feed slurry and sodium silicate depressant solution were continuously pumped into the sodium silicate conditioning tank for 2 minutes of conditioning. After sodium silicate conditioning, the feed slurry was pumped to the starch conditioning tank for 1 minute of further conditioning. The depressant conditioned feed slurry and apatite collector were then pumped into the final collector conditioning tank. Finally, the collector conditioned feed was pumped to a rougher column cell using a peristaltic pump. The conditioning time within each conditioning stage was

Table 2. Three-factor three-level central composite design

Test		Factors and Levels		
Std	Run	A Washwater	B Feed P_{80}	C Feed Solids
13	1	0	0	0
3	2	-1	1	0
9	3	0	-1	-1
16	4	0	0	0
10	5	0	1	-1
15	6	0	0	0
8	7	1	0	1
17	8	0	0	0
4	9	1	1	0
7	10	-1	0	1
12	11	0	1	1
6	12	1	0	-1
1	13	-1	-1	0
14	14	0	0	0
5	15	-1	0	-1
11	16	0	-1	1
2	17	1	-1	0

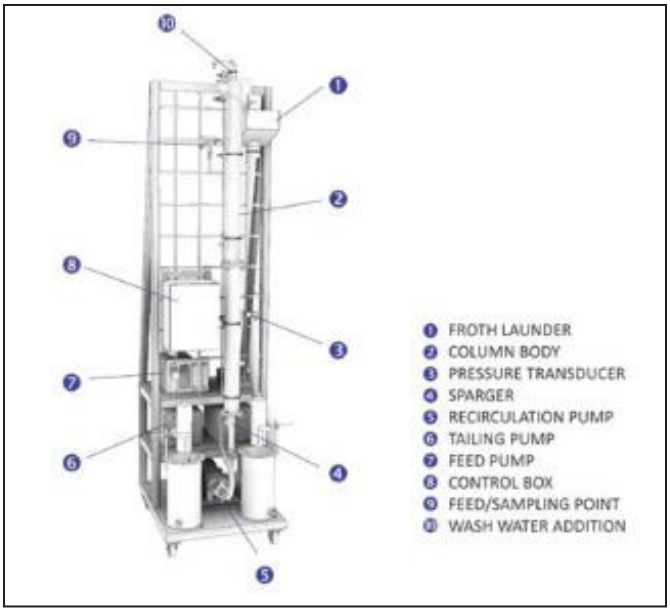

Figure 2. Schematic of Eriez lab flotation column

calculated by dividing the effective volume of the slurry in the conditioning tank by the volumetric flow rate.

During investigation of the column flotation responses of all feedstocks, the wash water rate, flotation feed solids content, and feed particle size (P_{80}) were adjusted based on the experiment design shown in Table 1 and Table 2. Once steady-state conditions were obtained, timed samples of the feed, overflow and underflow were collected. The slurry samples were then filtered, dried, weighed, and split for assay by ARL™ PERFORM'X sequential X-Ray fluorescence spectrometer. Measured mass yields and sample assays were used to perform a mass balance on each set of samples taken under a given set of test conditions. The mass balances were reconciled using a sum of squares minimization algorithm on the error residuals.

RESULTS AND DISCUSSIONS

Ultrafine Particles and Bubble Attachment

One major problem for ultrafine phosphate flotation is the low flotation probability. This is because of

- the low probability of bubble-particle collision due to the limited inertia of ultrafine particles to penetrate streamlines and collide with bubbles;
- the low probability of bubble-particle adhesion because of the short of particles' sliding time on bubble surface upon bubble-particle collision.

Figure 3 displays the microscopic observations of ultrafine phosphate particles successfully attached to fine and ultrafine bubbles generated by Eriez' CavTube sparger. It can be seen from this microscopic photo that coagulation and flocculation occurred in this ultrafine ore slurry after being treated by Eriez' CavTube sparger, which significantly improved the ultrafine phosphate flotation probability. This flotation probability can be further increased by using gum or starch. A previous study [88] found that fine guar gum/starch particles readily attached to fine bubbles as a result of generally negatively charged bubbles [5–6, 89–90] and positively charged cationic guar gum particles.

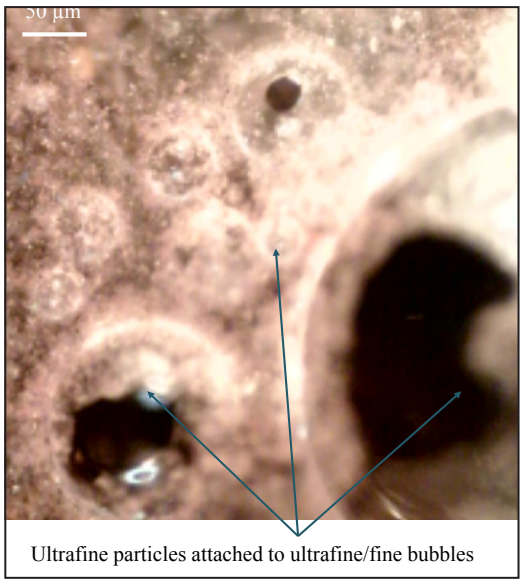

Figure 3. Ultrafine phosphate particle flotation

Ultrafine Gangue Minerals Entrainment

Figure 4 shows the ultrafine black and red iron oxides entrained during benchtop mechanical cell ultrafine phosphate direct flotation. Figure 5 presents the microscopic observations of ultrafine iron oxide particles entrained to froth phosphate product during benchtop mechanical cell flotation.

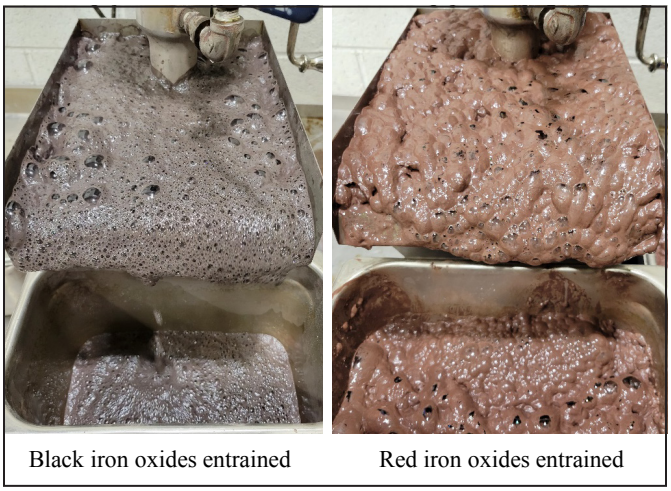

Figure 4. Ultrafine black and red iron oxides entrained during benchtop mechanical cell flotation

Hydraulic entrained gangue minerals are generally proportional to feed water recovered in froth product, which can be reduced using deep froth or wash water. Figure 6 shows that the froth zone becomes whiter and the interface between the collection zone and froth zone becomes clearer as the flotation column wash water rate increases from 0 liter/minute to 400 liter/minute and 800 liter/minute. The wash water used in flotation column provides the bias water and the water necessary to overflow the collected solids into the concentrate launder. The bias water replaces the water naturally draining from the froth, which tends to promote froth stability and can increase froth height. Therefore, the wash water can reduce entrained gangue minerals by decreasing feed water to froth product and increasing froth depth.

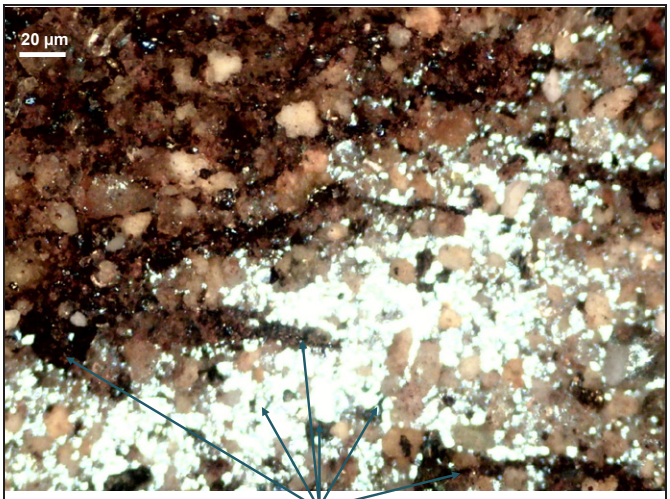

Figure 5. Microscopic observations of ultrafine iron oxide particles entrained to froth product during benchtop mechanical cell flotation

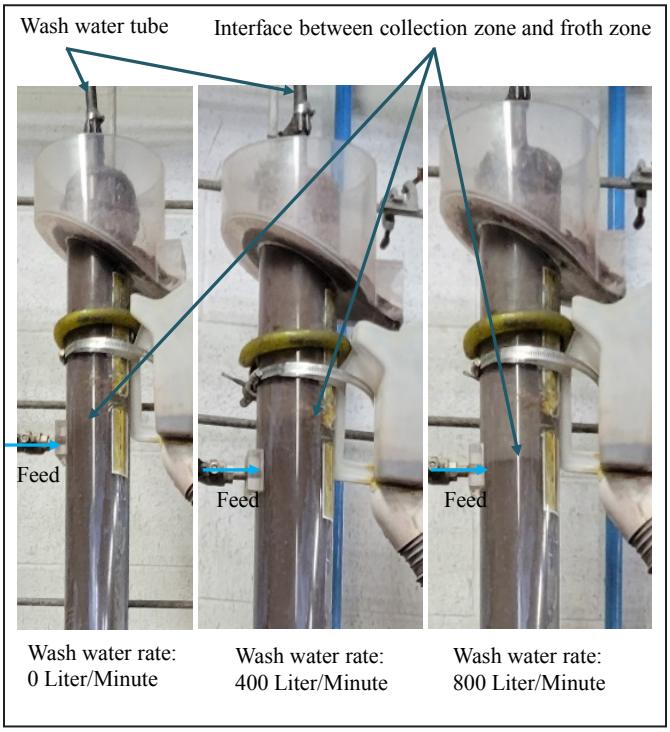

Figure 6. Column froth with various wash water rate

Figure 7 and Figure 8 display the microscopic observations of froth without wash water and with wash water. In Figure 7, entrained black and red iron oxides gangue minerals were reduced by using wash water; in Figure 8, the entrainment of silica gangue minerals was effectively reduced by wash water.

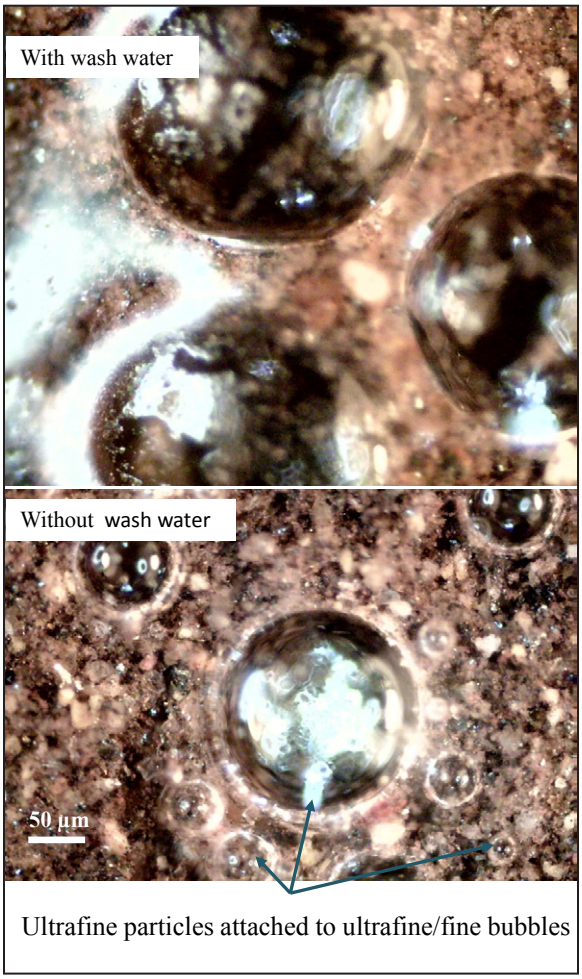

Figure 7. Microscopic observations of froth without wash water and with wash water. Entrained black and red iron oxides reduced by wash water

Three-Factor Three-Level Central Composite Design

Table 3. is offered to summarize the three-factor three-level central composite design experiment flotation results. Response surface methodology was used to analyze the three-factor (wash water rate, feed slurry solids content, and feed particle size) three-level central composite ultrafine phosphate column flotation experiment data. Response surface, cubic graph and contours were generated for the floated concentrate P_2O_5 grade and the floated concentrate P_2O_5 recovery as a function of three process parameters included wash water flow rate, feed slurry solids content, and feed particle size (P_{80}).

Figure 9 illustrates the effects of wash water flow rate and feed particle size (P_{80}) on the floated concentrate P_2O_5 grade. As shown in Figure 9, the middle level particle size (P_{80}=38 microns) feed floated concentrate P_2O_5 grade significantly increases from approximately 16% P_2O_5 to around 24% P_2O_5 and 30% P_2O_5 as the wash water flow

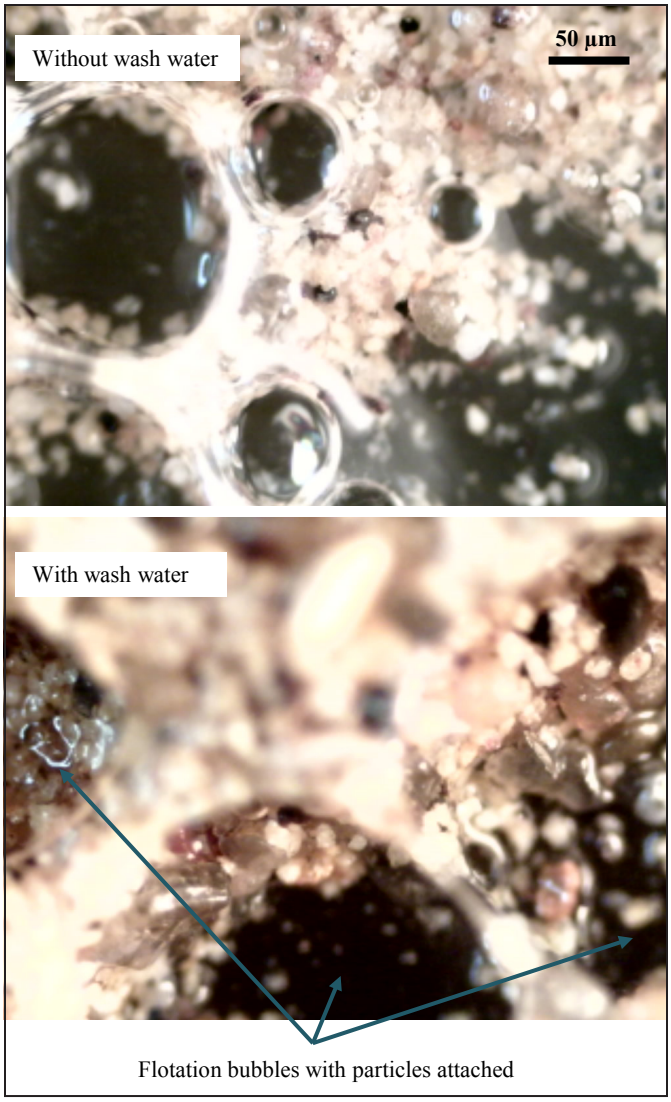

Figure 8. Microscopic observations of froth without wash water and with wash water. Entrained silica reduced by wash water

rate increases from 0 liter/minute to 400 liter/minute and 800 liter/minutes, respectively. The addition of wash water to flotation column froth zone can minimize the unwanted gangue mineral particles entrained. The floated concentrate P_2O_5 grade slightly increases when the flotation feed particle size (P_{80}) increases from 20 microns to 38 microns and 53 microns. This is because the entrained gangue minerals particles decrease as the increasing of flotation feed particle size (P_{80}).

Figure 10 displays the effects of feed slurry solids content and wash water flow rate on the floated concentrate P_2O_5 grade. As shown in Figure 10, the wash water rate has a far more significant effect on the improvement of the floated concentrate P_2O_5 grade than the flotation feed

Table 3. Three-factor three-level central composite design flotation results

Run	Feed P_2O_5 (%)	Concentrate P_2O_5 (%)	Tailings P_2O_5 (%)	Mass Yield (%)	P_2O_5 Recovery (%)
1	9.8	28.80	1.2	31.16	91.57
2	10.8	19.28	1.4	52.57	93.85
3	8.8	22.20	1.5	35.27	88.97
4	9.8	28.90	1.2	31.05	91.56
5	10.8	26.80	1.4	37.01	91.83
6	9.8	29.20	1.2	30.71	91.52
7	9.8	30.10	1.86	28.12	86.36
8	9.8	29.10	1.2	30.82	91.53
9	10.8	31.60	1.5	30.90	90.40
10	9.8	15.70	1.74	57.74	92.50
11	10.8	25.30	2.04	37.66	88.22
12	9.8	30.70	1.3	28.91	90.57
13	8.8	15.10	0.9	55.63	95.46
14	9.8	29.00	1.2	30.94	91.54
15	9.8	16.80	1.3	54.84	94.01
16	8.8	20.50	1.56	38.23	89.05
17	8.8	28.90	1.02	27.91	91.64

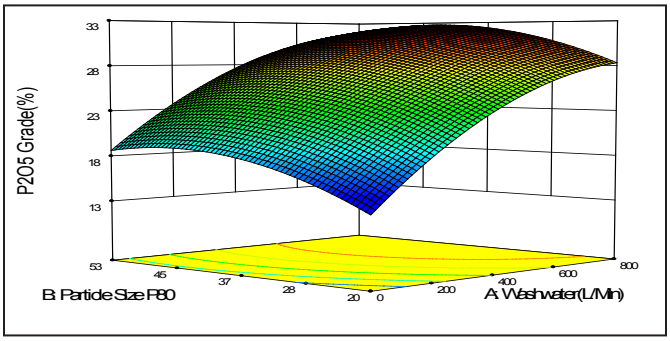

Figure 9. Concentrate P_2O_5 grade vs wash water rate and feed particle size P_{80}

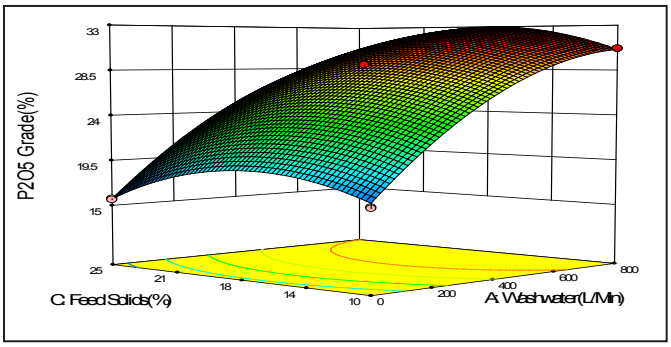

Figure 10. Floated concentrate P_2O_5 grade vs wash water rate and feed slurry solids content

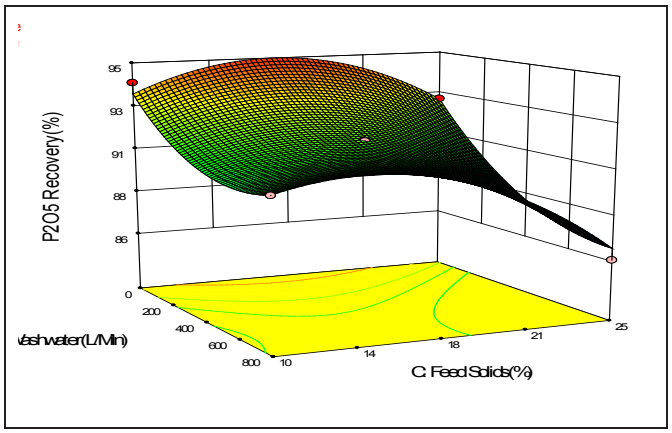

Figure 11. Floated concentrate P_2O_5 recovery vs wash water rate and feed slurry solids content

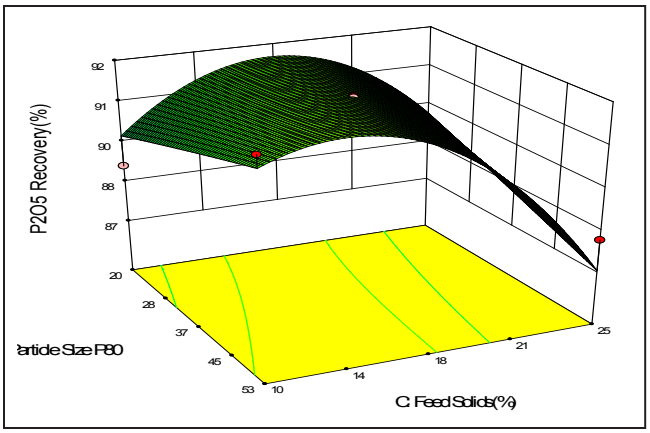

Figure 12. Floated concentrate P_2O_5 recovery vs feed particle size and feed slurry solids content

solids content. The highest floated concentrate P_2O_5 grade was achieved at the middle level feed slurry solids content 17.5%, below or above which the floated concentrate P_2O_5 grade drops slightly. This is because the entrained gangue minerals were reduced when the feed slurry percent solids decreased from high level 25% to middle level 17.5%. However, the further decreasing of the feed slurry solids content from middle level 17.5% to low level 10% will increase the feed water recovered in froth product, which is generally proportional to hydraulic gangue minerals entrainment. Another possible reason, the amount of relatively coarse high P_2O_5 grade phosphate particles were more easily lost to nonfloated tailings at the low-level feed solids slurry, which decreased the floated concentrate P_2O_5 grade.

Figure 11 depicts the effects of wash water flow rate and feed slurry solids content on the floated concentrate P_2O_5 recovery. The results given in Figure 11 show that the highest floated concentrate P_2O_5 recovery was achieved at the middle-level feed percent solids 17.5% and the low-level wash water rate. The flotation P_2O_5 recovery slightly decreases with the increasing of the flotation feed slurry solids content from middle-level 17.5% to high-level 25%, and the decreasing of the flotation feed slurry solids content from middle-level 17.5% to low-level 10%. The increase in wash water rate to minimize the unwanted gangue mineral particles entrainment can reject some unliberated phosphate/gangue middling particles and thus slightly decrease the flotation recovery. Therefore, the optimized process operation conditions are to control the balance between **a** *high* recovery of the *desired* P_2O_5 and a high-grade P_2O_5 value of the phosphate concentrate.

Figure 12 shows the effects of feed slurry solids content and flotation feed particle size (P_{80}) on the floated concentrate P_2O_5 recovery. The floated concentrate P_2O_5 recovery increases when the flotation feed particle size (P_{80}) decreases from 53 microns to 38 microns and 20 microns. The floated concentrate P_2O_5 recovery drops more sharply for coarser flotation feed than finer feed when the flotation feed percent solids increases from middle-level 17.5% to 25%.

Laboratory Column and Mechanical Cell Flotation

Following the completion of benchtop mechanical cell and laboratory column optimization testing, benchtop mechanical cell flotation under optimized conditions and column flotation were conducted on various ultrafine phosphate slime samples.

Figure 13 is offered to summarize the P_2O_5 grade and recovery relationships for the optimal bench-top mechanical cell and column flotation results realized from treatment of a 38x0 micron ultrafine phosphate slime. The

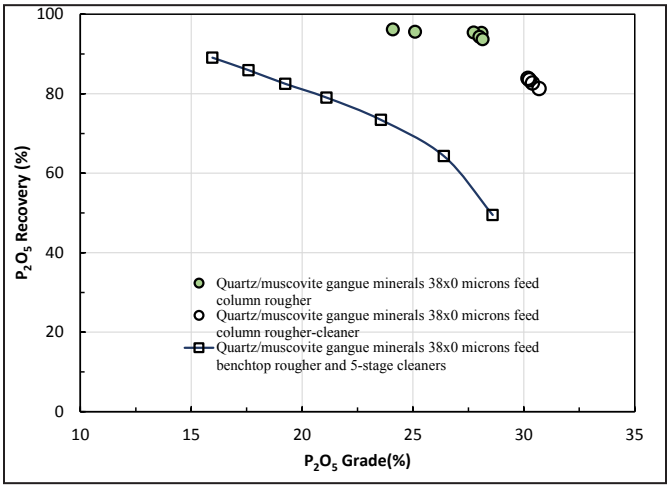

Figure 13. Flotation column vs benchtop mechanical cell

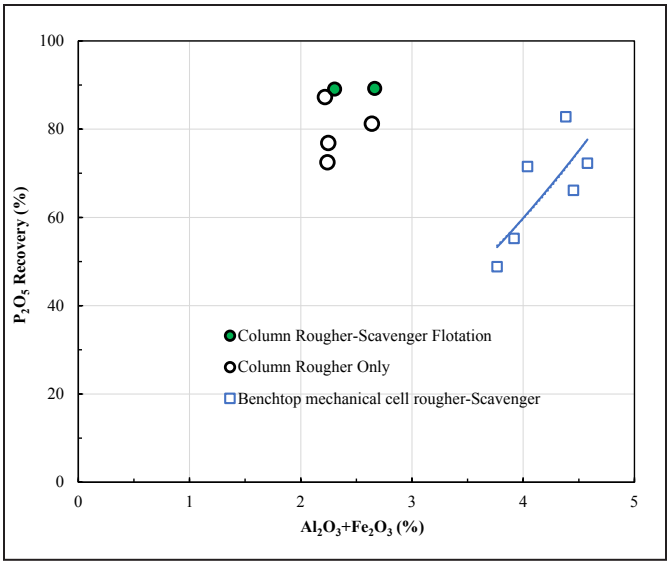

Figure 14. Flotation column vs benchtop mechanical cell

gangue minerals of this ultrafine phosphate slime sample were mainly composed of quartz and muscovite. As demonstrated by the grade-recovery relationships in Figure 13, significantly improved flotation performance was achieved used column rougher and rougher-cleaner flotation versus mechanical cell rougher and 5-stage cleaner flotation. As a result of the use of cavitation-tube sparger, wash water and a deep froth phase, high recoveries were maintained at much improved product grades.

Figure 14 displays the phosphate concentrate gangue [Al_2O_3+Fe_2O_3] content and P_2O_5 recovery relationships for the optimal bench-top and column flotation tests performed on the Industries Chimiques du Senegal (ICS) ultrafine slime tailings, a concentrate grade of 2.3% [Al_2O_3+Fe_2O_3] and 36.0% P_2O_5 was achieved at 89.4% P_2O_5 recovery. As illustrated by the grade-recovery relationships in Figure 14, an obviously higher flotation P_2O_5 recovery and lower [Al_2O_3+Fe_2O_3] content was achieved using column flotation than benchtop mechanical flotation. High amounts of [Al_2O_3+Fe_2O_3] in the phosphate concentrate product will decrease the next stage wet process plant capacity and phosphoric acid recovery. Generally, less than 2–3% of [Al_2O_3+Fe_2O_3] is desired.

Both Figure 13 and Figure 14 demonstrate that cavitation-tube flotation columns are superior to conventional mechanical cells. In addition to lower ultrafine gangue particle entrainment, the ultrafine bubble selectively flocculated ultrafine/fine phosphate particles encountered less turbulence in the collection zone near the column flotation feed point than in mechanical cell flotation, preventing the break-up of formed phosphate particle flocs. Cavitation tube generated fine and ultrafine bubbles can assist fine hydrophobic particles to form flocs and thus improve fine/ultrafine particle flotation kinetics and selectivity.

SUMMARY AND CONCLUSIONS

Microscopic observations of ultrafine phosphate slime flotation froth with and without wash water demonstrate that the entrained ultrafine gangue minerals such as iron oxide, quartz, and muscovite particles can be minimized by using wash water in column flotation.

In the three-factor (wash water rate, feed slurry solids content, and feed particle size) three-level central composite design experiment flotation tests, the best flotation results were achieved at the middle-level feed solids content (17.5%) and middle to high level wash water rate (400–800 liter/minute).

Improved flotation performance was achieved for both various ultrafine phosphate slime samples using column flotation as compared to benchtop mechanical flotation. The enhanced flotation performance was because of the use of cavitation-tube sparger, wash water and a deep froth phase in column flotation.

REFERENCES

[1] Kohmuench J, Christodoulou L, Fan M M, Mankosa M, Luttrell G (2010) Advancements in coarse and fine particle flotation. In: Proceedings of the 42nd Annual Canadian Mineral Processors Operators Conference, Ontario, Canadian Mineral Processors, pp.55–69.

[2] Wyslouzil H, Kohmeunch J, Christodoulou L, Fan M M (2009) Coarse and fine particle flotation, COM 2009, 48th Conference of Metallurgists, August 23–26, Sudbury, Ontario.

[3] Wasmund E B (2014) Flotation technology for coarse and fine particle recovery. I Congreso Internacional De Flotacion De Minerales. Lima, Peru Aug 2014.

[4] Fan M M, Tao D (2008) A Study on picobubble enhanced coarse phosphate froth flotation. Separation Science and Technology 43:1–10.

[5] Fan M M, Tao D, Honaker R, Luo Z F (2010) Nanobubble generation and its application in froth flotation (part I): nanobubble generation and its effects on properties of microbubble and millimeter scale bubble solutions. Mining Science and Technology (Now: Int J of Min Sci and Techn). 20(1):1–19.

[6] Fan M M, Tao D, Honaker R, Luo Z F (2010) Nanobubble generation and its application in froth flotation (part II): fundamental study and theoretical analysis. Mining Science and Technology 20(2):159–177.

[7] Fan M M, Tao D, Honaker R, Luo Z F (2010) Nanobubble generation and its application in froth flotation (part III): specially designed laboratory scale column flotation of phosphate. Mining Science and Technology 20(3):317–338.
[8] Fan M M, Tao D, Honaker R, Luo Z F (2010) Nanobubble generation and its application in froth flotation (part IV): mechanical cells and specially designed column flotation of coal. Mining Science and Technology 20 (5):641–671.
[9] Liu B, Manica R, Zhang X R, Bussonnière A, Xu Z H, Xie G Y (2018) Dynamic interaction between a millimeter-sized bubble and surface microbubbles in water. Langmuir 34(39):11667–11675.
[10] Peng H, Hampton M A, Nguyen A V (2013) Nanobubbles do not sit alone at the solid-liquid interface. Langmuir 29 (20):6123–30.
[11] Zhou Z A, Xu Z, Finch J A, Hu H, Rao S R (1997) Role of hydrodynamic cavitation in fine particle flotation. Int J of Mineral Processing 51:139–149.
[12] Calgaroto S, Wilberg K, Rubio J (2014) On the nanobubbles interfacial properties and future applications in flotation. Miner Eng 60:33–40.
[13] Li C W, Zhang H J (2022) A review of bulk nanobubbles and their roles in flotation of fine particles. Powder Technology 395: 618–633.
[14] Zhou W, Wu C, Lv H, Zhao B, Liu K, Ou L (2020) Nanobubbles heterogeneous nucleation induced by temperature rise and its influence on minerals flotation. Applied Surface Science 508:145282.
[15] Tao D, Wu Z, Sobhy A (2021) Investigation of nanobubble enhanced reverse anionic flotation of hematite and associated mechanisms. Powder Technology 379:12–25.
[16] Pourkarimi Z, Rezai B, Noaparast M., Chehreh Chelgani S, Nguyen A V (2021) Proving the existence of nanobubbles produced by hydrodynamic cavitation and their significant effects in powder flotation. Advanced Powder Technology 32(4).
[17] Zhang F, Sun L, Yang H, Gui X, Schönherr H, Kappl M, Cao Y J, Xing Y W (2021) Recent advances for understanding the role of nanobubbles in particles flotation. Advances in Colloid and Interface Science 291:102403.
[18] Cheng G, Zhang M N, Li Y L, Lau E V (2023) Improving micro-fine mineral flotation via micro/nano technologies. Separation Science and Technology 58(3):520–537.
[19] Chang Z, Niu S, Shen Z, Zou L, Wang H (2023) Latest advances and progress in the microbubble flotation of fine minerals: Microbubble preparation, equipment, and applications. International Journal of Minerals, Metallurgy and Materials, Volume 30, pages 1244–1260.
[20] Asgari K, Khoshdast H, Nakhaei F, Garmsiri M R, Huang Q Q, Hassanzadeh A (2023) A review on floc-flotation of fine particles: Technological aspects, mechanisms, and future perspectives. Mineral Processing and Extractive Metallurgy Review, July 2023, doi.org/10.1080/08827508.2023.2236770.
[21] Hang H (2018) The mechanism of floc formation by hydrodynamic cavitation and its application on fine particle flotation. M.S. Thesis, Department of Chemical and Materials Engineering, University of Alberta.
[22] W Zhou, H Chen, L Ou, Q Shi (2016) Aggregation of ultra-fine scheelite particles induced by hydrodynamic cavitation. Int. J of Mineral Proc 157(10): 236–240.
[23] Jeong Y A, Poddar M K, Ryu H Y, Yerriboina N P, Kim T G, Kim J H, Park J D, Lee M G, Park C Y, Han S J, Kim, M J, Park J G (2019) Investigation of particle agglomeration with in-situ generation of oxygen bubble during the tungsten chemical mechanical polishing (CMP) process. Microelectronic Eng 218:111133.
[24] Hassanzadeh A, Firouzi M, Albijanic B, Celik M S (2018) A review on determination of particle–bubble encounter using analytical, experimental and numerical methods. Minerals Eng 122(15):296–311.
[25] Liu B, Manica R, Zhang X R, Bussonnière A, Xu Z H, Xie G Y (2018) Dynamic interaction between a millimeter-sized bubble and surface microbubbles in water. Langmuir 34(39):11667–11675.
[26] Wang Y, Luo X, Qin W, Jiao F (2019) New insights into the contact angle and formation process of nanobubbles based online tension and pinning. Applied Surface Science 481(1):1585–1594.
[27] Nirmalkar N, Pacek A W, Barigou M (2018) Interpreting the interfacial and colloidal stability of bulk nanobubbles. Soft Matter (14): 9643–9656.
[28] Anzoom S J, Bournival G, Seher Ata S (2024) Coarse particle flotation: A review. Minerals Engineering 206 (2024) 108499.
[29] Nazari S, Shafaei S Z, Gharabaghi M, Ahmadi R, Shahbazi B, Fan M M (2019) Effects of nanobubble and hydrodynamic parameters on coarse quartz flotation. Int J of Mining Science and Technology 29(2):289–295.

[30] Rosa A F, Rubio J (2018) On the role of nanobubbles in particle–bubble adhesion for the flotation of quartz and apatitic minerals. Minerals Eng (127): 178–184.
[31] Nazari S, Gholami A, Khoshdast H, Li J L , He Y Q, and Hassanzadeh A (2023) Advanced simulation of quartz flotation using micro-nanobubbles by hybrid serving of historical data (HD) and deep learning (DL) methods. Minerals 2023, 13, 128.
[32] Chipakwe V, Karlkvist T, Rosenkranz J, Chelgani S C (2023) Exploring the effect of a polyacrylic acid-based grinding aid on magnetite-quartz flotation separation. Separation and Purification Technology 305 (2023) 122530.
[33] Chipili C, Bhondayi C (2023) Bubble loading in a fluidized column: effects of bubble size, particle size, contact angle and particle density. Mineral Processing and Extractive Metallurgy Review, 1–13.
[34] Ahmadi R, Darban A K, Abdollahy M, Fan M M (2014) Nano-microbubble flotation of fine and ultrafine chalcopyrite particles. J Min Sci Technol 24:559–66.
[35] Rulyov N, Nessipbay T, Dulatbek T, Larissa S, Zhamikhan K (2018) Effect of microbubbles as flotation carriers on fine sulphide ore beneficiation. Mineral Process and Extractive Metall 127 (3):133–139.
[36] Chipakwe V., Sandb A, Chelgani S C (2021) Nanobubble assisted flotation separation of complex Pb–Cu–Zn sulfide ore—Assessment of process readiness. Separation Science and Technology 1–9.
[37] Fan M, Milbourne J, Hobert A, Letkiewicz R (2023) Enhanced flotation of ultrafine copper/gold/silver minerals using optimized reagent schemes and Eriez column/Stackcell high-intensity flotation technologies. SME Annual Conference Feb. 26 - Mar. 01, 2023, Denver, CO.
[38] Kazemi F , Bahrami A, Ghorbani Y , Danesh A , Abdollahi M, Falah H , Salehi M (2023) The interaction and synergic effect of particle size on flotation efficiency: A comparison study of recovery by size, and by liberation between lab and industrial scale data. Rudarsko-geološko-naftni zbornik (The Mining-Geology-Petroleum Engineering Bulletin) UDC: 622–699.
[39] Mahani A N, Karamoozian M, Chegeni M J, Meymand M M (2023) Effect of stable nano-microbubbles on sulfide copper flotation and reduction of chemicals dosage. Journal of Mining and Environment (JME), jme.shahroodut.ac.ir/article_2848.html.
[40] Zinjenab Z T, Azimi E, Shadman M, Hosseini M R, Abbaszadeh M, Namgar S M (2023) Nano-microbubbles and feed size interaction in lead and zinc sulfide minerals flotation. Chemical Engineering and Processing - Process Intensification, Volume 189, July 2023, 109401.
[41] Shadman M, Hosseini M R, Zinjenab Z T, Azimi E (2023) Significant reduction in collector consumption by implementing ultrafine bubbles in lead and zinc rougher flotation. Powder Technology, Volume 414, 118096.
[42] Fan M M, Tao D (2012) A pilot-scale study of effects of nanobubbles on phosphate flotation. In: Zhang P, Miller J D, El-Shall H E, editors. Beneficiation of phosphates: new thought, new technology, new development. Littleton (CO): Soc for Min, Metall, and Explor; pp. 21–31.
[43] Hobert A, Dohm E, Tallarico F, Dede (2019) Improved flotation recovery and selectivity of an ultra-fine Brazilian phosphate ore using Eriez' column flotation technology. SYMPHOS 2019.
[44] Reis A S, Reis F A M, Demuner L R, Barrozo M A S (2019) Effect of bubble size on the performance flotation of fine particles of a low-grade Brazilian apatite ore. Powder Tech. 356:884–891.
[45] Nakhaie F (2023) Application of nano bubbles in column flotation: Beneficiation of iron and phosphate slimes. Conference: IMCET 2022 / ANTALYA / TURKEY / March 22—25.
[46] Reis A S, Mendes T F, Júnior I P, Barrozo M A (2023) Influence of bubble size on performance of apatite flotation of different particle sizes. Particulate Science and Technology, Volume 41, Issue 7, Pages 1044–1052.
[47] Fan M M, Zhao Y, Tao D (2012) Fundamental studies of nanobubble generation and applications in flotation. In: Separation Technologies for Minerals, Coal, and Earth Resources, Society for Mining, Metallurgy, and Exploration, Littleton, CO, pp.457–469.
[48] Fan M M, Tao D, Zhao Y M, Honaker R (2013) Effect of nanobubbles on the flotation of different sizes of coal particle. Minerals and Metallurgical Processing 30 (3):157–167.
[49] Tao D, Fan M M (2010) Enhanced fine coal column flotation using cavitation concept. Proceedings of XVI International Coal Preparation Congress. Society for Mining, Metallurgy, and Exploration. PP: 413–420.
[50] Fan M M, Tao D (2014) Effect of nanobubbles on flotation of different density coal. 2014 SME Annual Meeting, February 23 –26, Salt Lake City, Utah.

[51] Wang School of Chemical Engineering and Technology, China University of Mining & Technology, Xuzhou, Jiangsu, China Y W, Xing School of Chemical Engineering and Technology, China University of Mining & Technology, Xuzhou, Jiangsu, China Y W, Gui X H, Cao Y J, Xu National Engineering Research Center of Coal Preparation and Purification, Xuzhou, Jiangsu, China X H (2018) The characterization of flotation selectivity of different size coal fractions. International Journal of Coal Preparation and Utilization. 38(7):337–354National Engineering Research Center of Coal Preparation and Purification, Xuzhou, Jiangsu, ChinaCorrespondenceguixiahui1985 @163.com.

[52] Felicia F P, Yu X (2015) Pico–nano bubble column flotation using static mixer-venturi tube for Pittsburgh No. 8 coal seam. Int J of Min Sci and Tech 25 (3):347–354.

[53] Ebrahimi H, Karamoozian M, Saghravani S F (2020) Interaction of applying stable micro-nano bubbles and ultrasonic irradiation in coal flotation. Int. J. of Coal Preparation and Utilization 40(2): 1–15.

[54] Li P W, Zhang M, Wang L, Wei Y, Fan R (2020) Effect of nanobubbles on the slime coating of kaolinite in coal flotation. ACS omega 5 (38): 24773–24779.

[55] Han H, Liu A, Wang H F (2020) Effect of hydrodynamic cavitation assistance on different stages of coal flotation. Minerals 10(3):221.

[56] Ma F Y, Tao D P, Tao Y J, Liu S Y (2021) An innovative flake graphite upgrading process based on HPGR, stirred grinding mill, and nanobubble column flotation. Int. J. of Mining Science and Technology 31: 1046–1055.

[57] Tang C L, Ma F Y, Wu TY, Zhang D, Wang Y, Zh ao T L, Fan Z L, Liu X Y (2023) Study on surface physical and chemical mechanism of nanobubble enhanced flotation of fine graphite. Journal of Industrial and Engineering Chemistry, Volume 122, Pages 389–396.

[58] Ma F, Tao D (2023) A study of mechanisms of nanobubble-enhanced flotation of graphite. Nanomaterials 2022, 12(19), 3361.

[59] Zhang D, Ma F, Tao Y (2023) Study on effect of nanobubble on ultra-fine flake graphite (UFG) flotation. Particulate Science and Technology. Volume 41, 2023 - Issue 7, Pages 1062–1070.

[60] Wang Y F, Pan Z C, Luo X M, Qin W Q, Jiao F (2019) Effect of nanobubbles on adsorption of sodium oleate on calcite surface. Minerals Eng 133 (15): 127–137.

[61] Zhou J Z, Li H H, Chow R S, Liu Q X, Xu Z H, Masliyah J (2019) Role of mineral flotation technology in improving bitumen extraction from mined Athabasca oil sands—II. Flotation hydrodynamics of water-based oil sand extraction. The Canadian Journal of Chemical Engineer 97(7):1–23.

[62] Li W, Lin H, Yang Y, Shang Z, Li Q, Ma Y, Liu A, Jiang M (2021) Enhanced separation of oil and solids in oily sludge by froth flotation at normal temperature. Processes 9(12):2163.

[63] Etchepare R, Oliveira H, Azevedo A, Rubio J (2017) Separation of emulsified crude oil in saline water by dissolved air flotation with micro and nanobubbles. Sep Purif Technol 186:326–32.

[64] Lim M W, Lau E V, Poh P E (2018) Micro-macrobubbles interactions and its application in flotation technology for the recovery of high-density oil from contaminated sands. J of Petroleum Science and Engineering 161:29–37.

[65] Wang C, Lü Y, C Song C, Zhang D, Rong F, He L (2022) Separation of emulsified crude oil from produced water by gas flotation: A review. 845: 157304.

[66] Colic M (2024) The influence of various parameters on petroleum oil removal from produced water with novel nanobubbles/microbubbles flotation. International Petroleum Technology Conference, IPTC, 12–14 February 2024, Dhahran Expo. Paper Number (IPTC-24290-MS.

[67] Lin F (2023) Design and construction of a continuous pilot flotation facility: A case study for water-based oil sand extraction. Petroleum Research 8 (2023) 309–315.

[68] Zhou W, Niu J, Xiao W, Ou L (2019) Adsorption of bulk nanobubbles on the chemically surface-modified muscovite minerals. Ultrasonics sonochemistry 51: 31–39.

[69] Shao H, Li P, Sobhy A, Ling X, Tao D, Zhang M (2023) Effects of pure and modified nanobubbles on the reverse flotation of kaolinite from hematite. Mineral Processing and Extractive Metallurgy Review (IF 5) Published online: doi.org/10.1080/08827508.2023.2260932.

[70] Wei P, Ren L, Zhang Y, Bao S (2021) Influence of microbubble on fine wolframite flotation. Minerals 11(1079), Page 1–13.

[71] Tsave P K, Kostoglou M, Karapantsios T D, Lazaridis N K (2023) Enhancing fines recovery by hybrid

flotation column and mixed collectors. Minerals, 2023, 13 (7):849.
[72] Taguta J, Safari M, Govender V, Chetty D (2023) Investigating the amenability of a PGM-bearing ore to coarse particle flotation. Minerals 2023, 13, 698.
[73] Capponi F, Azevedo A, Oliveira H, Rubio J (2023) Column rougher flotation of fine niobium-bearing particles assisted with micro and nanobubbles. Minerals Engineering, Volume 199, 108119.
[74] Lu B, Xu W, Luo C, Li W, Su X, Song Y, Zhou J and Li K (2023) Effect of nanobubbles on the flotation behavior of microfine-grained serpentine. Minerals 2023, 13, 1299.
[75] Hashim M A, Mukhopadhyay S, Gupta B S, Sahu J N (2012) Application of colloidal gas aphrons for pollution remediation. J Chem Technol Biotechnol 87:305–24.
[76] Reyes R, Flores J V (2017) Efficiency of micro-nanobubbles for wastewater treatment in puerto bermúdez, oxapampa, pasco. Journal of Nanotechnology 1(1): 18–24.
[77] Shi Y, Yang J, Ma J, Luo C (2017) Feasibility of bubble surface modification for natural organic matter removal from river water using dissolved air flotation. Frontiers of Environmental Science & Engineering 11: 10.
[78] Temesgem T, Bui T T, Han M Y, Kim T I, Park H J (2017) Micro and nanobubble technologies as a new horizon for water-treatment techniques: A review. Advances in Colloid and Interface Science 246: 40–51.
[79] Uchida T, Oshita S, Ohmori M, Tsuno T, Soejima K, Shinozaki S, et al (2011) Transmission electron microscopic observations of nanobubbles and their capture impurities in wastewater. Nanoscale Res Lett 6. 295:1–9.
[80] Senthilkumar G and SL Sankar SL (2023) Implementation of micro-nanobubbles technology for the treatment of domestic wastewater: experimental study. Water, Air, & Soil Pollution, 234, 46 (2023).
[81] He Y, Zhang T, Lv L, Tang W, Wang Y, Zhou J, Tang S (2023) Application of microbubbles in chemistry, wastewater treatment, medicine, cosmetics, and agriculture: a review. Environmental Chemistry Letters volume 21, pages 3245–3271.
[82] Wang Z, An C, Lee K, Feng Q, Zhang B (2023) Exploring the role of nanobubbles in the fate and transport of spilled oil on shorelines. ACS EST Water 2023, 3, 1, 30–40.
[83] Kamei T, Tsutsumi Y, Rujakom S, Eamrat R, Kazama F (2023) Hydrogenotrophic denitrification for treatment of nitrate-contaminated groundwater: Using a microbubble diffuser to optimize performance. Journal of Water Process Engineering 55 (2023) 104062 .
[84] Marcelino K R, Ling L, Wongkiew S, Nhan H T, Surendra K. C., Shitanaka T, Lu H, Khanal S K (2023) Nanobubble technology applications in environmental and agricultural systems: Opportunities and challenges. Critical Reviews in Environmental Science and Technology, Volume 53, 2023 - Issue 14, Pages 1378–1403.
[85] Kumar S (2023) Smart and innovative nanotechnology applications for water purification. Hybrid Advances, Volume 3, August 2023, 100044.
[86] Huang H, Yang X, Wu Z , Qiao B, Ma G, Shao H, Tao D (2023) An investigation of nanobubble enhanced flotation for fly ash decarbonization. Colloids and Surfaces A: Physicochemical and Engineering Aspects, Volume 679, 132563.
[87] Nazari S, Li J L, Khoshdast H, Li J H, Ye C L, He Y Q, Hassanzadeh A (2023) Effect of roasting pretreatment on micro-nanobubble-assisted flotation of spent lithium-ion batteries. Journal of Materials Research and Technology, Volume 24, Pages 2113–2128.
[88] Fan M M, Hobert D (2022) Fundamentals and applications of green modifiers for froth flotation. Mining, Metallurgy & Exploration, Vol. 39, Pages 39–48.
[89] Alheshibri M H (2019) Nanobubbles in bulk. Ph D dissertation. Research School of Physics and Eng, The Australian National University.
[90] Azevedo A, Oliveira H, Rubio J (2019) Bulk nanobubbles in the mineral and environmental areas: Updating research and applications. Advances in Colloid and Interface Science 271:101992.
[91] Zhou S, Nazari S, Hassanzadeh A, Bu X, Ni C, Peng Y, Xie G, He Y (2022) The effect of preparation time and aeration rate on the properties of bulk micro-nanobubble water using hydrodynamic cavitation. Ultrasonics Sonochemistry 84, 105965 Page 1–9.
[92] Zhang R, Gao Y, Chen L, Ge G (2022) Nanobubble boundary layer thickness quantified by solvent relaxation NMR. Journal of Colloid and Interface Science 609, Page 637–644.
[93] Bu X, Zhou S, Tian X, Ni C, Nazari S, Alheshibricd M (2022) Effect of aging time, airflow rate, and nonionic surfactants on the surface tension of bulk nanobubbles water. Journal of Molecular Liquids 359, 119274.

[94] Zhang F, Yang H, Gui X, Guo H, Cao Y, Xing Y (2022) Interfacial nanobubbles on different hydrophobic surfaces and their effect on the interaction of inter-particles. Applied Surface Science 582, 152184.
[95] Han S, Lee S, Joung YS (2022) Long-term effect of nanobubbles generated by turbulent flow through diamond-pattern notches on liquid properties. Results in Engineering 14: 100375.
[96] Hu K, Luo L, Sun X, Li H (2022) Unraveling the effects of gas species and surface wettability on morphology of interfacial nanobubbles. Nanoscale Advances 4: 2893–2901.
[97] Lee J I , Kim JM (2022) Influence of temperature on bulk nanobubble generation by ultrasonication. Colloid and Interface Science Communications 49: 100639.
[98] Zhang R, Gao Y, Chen L, Ge G (2022) Controllable preparation of monodisperse nanobubbles by membrane sieving. Colloids and Surfaces A: Physicochemical and Engineering Aspects 642: 128656.
[99] Bhoumick M C, Roy S, Mitra S (2022) Reduction and elimination of humic acid fouling in air sparged membrane distillation using nanocarbon immobilized membrane. Molecules 27(9):2896.
[100] Ulatowski K, Wierzchowski K, Fiuk J, Sobieszuk P (2022) Effect of nanobubble presence on murine fibroblasts and human leukemia cell cultures. Langmuir 38 (28): 8575–8584
[101] Bu X, Alheshibri M (2021) The effect of ultrasound on bulk and surface nanobubbles: A review of the current status. Ultrasonics sonochemistry 76:105629
[102] Wang S, Zhou L, Gao Y (2021) Can bulk nanobubbles be stabilized by electrostatic interaction? Physical Chemistry Chemical Physics 23 (31):16501–16505
[103] Wang S, Zhou L, Wang X, Hu J, Li P, Lin G, Gao Y, Zhang L, Wang C (2021) Collective dynamics of bulk nanobubbles with size-dependent surface tension. Langmuir, 37 (26): 7986–7994
[104] Li T, Cui Z, Sun J, Jiang C, Li G (2021) Generation of bulk nanobubbles by self-developed venturi-type circulation hydrodynamic cavitation device. Langmuir 37 (44): 12952–12960
[105] Doğan M, Bunyatova U, Ferhanoğlu O (2021) A new modeling approach for stability of micro/nano bubbles. IFAC-Papers OnLine 54 (14):144–148
[106] Ferraro G (2021) Understanding the stability and properties of bulk nanobubbles. Doctoral Thesis, etheses.bham.ac.uk › epriant. The University of Birmingham.
[107] Labarre L, Saint-Jalmes A, Vigolo D (2021) Microfluidics investigation of the effect of bulk nanobubbles on surfactant-stabilized foams. Colloids and Surfaces A: Physicochemical and Engineering Aspects 654,130169
[108] Yoon R H, Luttrell G H (1992) Development of the selective hydrophobic coagulation process. Report No. DOE/PC/91164-T1, Virginia Center for Coal and Minerals Processing, Blacksburg, VA (United States), 1992.

24-033

Enhancing Robotic Perception for Autonomous Roof Bolting Using an Event Based Machine Learning Framework

Akram Marseet
M3 Robotics Lab

Andrew J. Petruska
M3 Robotics Lab

Rik Banerjee
M3 Robotics Lab

ABSTRACT

Underground mine roof bolting is a crucial operation for miners' safety and mine sustainability. Since roof bolting is a manual or human-supervised operation, miners' safety is at risk due to dust or rock falls. Traditional machine learning algorithms have shown limitations to detecting drillable areas, mainly due to harsh lighting conditions. The authors propose an adaptive deep-learning framework for autonomous roof bolting. The proposed framework is based on implementing a binary semantic segmentation algorithm on color images to classify pixels that belong to rock from those that belong to non-rock. Significantly, the proposed framework implements deep learning semantic segmentation on images from traditional and neuromorphic vision sensors in underground mines. The performance of the proposed model shows an impressive accuracy level of at least 98% at a low number of training epochs with smooth learning curves. The high accuracy enables the implementation of autonomous roof bolting, greatly improving miners' safety and operational efficiency while reducing human exposure to safety hazards. This research will advance the use of deep learning in mining automation and has the potential to revolutionize the traditional mining industry.

INTRODUCTION

The Mining sector plays a pivotal role in the development of the world economy [1], [2]. Underground mining is growing due to the rising demand for minerals for industries such as the automotive industry and clean energy technologies [3]. Due to the rapid demand for minerals, the mining industry is moving toward deep underground mining [4]. Nonetheless, underground mining presents significant challenges across various dimensions [5]. Human safety is one of the main challenges in underground mining [6], mines sustainability [7], and working conditions [8] also contribute to other challenges in underground mining environments. According to a report issued by the United States Mine Safety and Health Administration (MSHA), the total number of fatal injuries till the third quarter of 2023 is higher than that for the previous year [9].

One of the hazards in the underground mining industry that causes fantails and serious injuries is falls on the roofs and the ribs of the underground mines. [10]. According to MSHA, 26 fatal injuries have been reported as of August 5th, 2023 [11]. Roof fall hazards are addressed by roof bolting [12] which has been recognized by the Coal Mine Health and Safety Act of 1969 as the exclusive method of providing support for underground entry [13]. Roof bolting is a fundamental technique for ensuring the safety and stability of underground mine environments, particularly in areas where roof conditions are unstable or prone to collapses [14]. Roof bolting is still an active research area where there are many aspects that need to be addressed including safety during roof bolting and increasing the efficiency of the roof bolting process. Roof bolting processes mainly include perforating the unsupported roof, followed by the insertion of a roof bolt and epoxy resin to fasten the overlying roof strata [15]. For rock support, straps are used [16]. Therefore, an additional step is added which is drilling through holes in the straps.

Although roof bolting improves the safety of mine personnel and the sustainability of mines, the roof bolting process is risky on roof blotters. There are safety hazards

This work is supported by National Institute for Occupational Safety & Health | NIOSH/Project 75D30121C12206.